UC Berkeley

UC Berkeley Previously Published Works

Title

Synthetic and Evolutionary Construction of a Chlorate-Reducing Shewanella oneidensis MR-1.

Permalink

https://escholarship.org/uc/item/63b758dq

Journal

mBio, 6(3)

ISSN

2150-7511

Authors

Clark, Iain C
Melnyk, Ryan A
Youngblut, Matthew D
et al.

Publication Date

2015-05-01

DOI

10.1128/mbio.00282-15

Peer reviewed

eScholarship.org Powered by the California Digital Library
University of California

RESEARCH ARTICLE

Synthetic and Evolutionary Construction of a Chlorate-Reducing *Shewanella oneidensis* MR-1

Iain C. Clark,[a] Ryan A. Melnyk,[b] Matthew D. Youngblut,[b] Hans K. Carlson,[b] Anthony T. Iavarone,[c] John D. Coates[b]

Department of Civil and Environmental Engineering, University of California, Berkeley, California, USA[a]; Department of Plant and Microbial Biology, University of California, Berkeley, California, USA[b]; QB3/Chemistry Mass Spectrometry Facility, University of California, Berkeley, California, USA[c]

ABSTRACT **Despite evidence for the prevalence of horizontal gene transfer of respiratory genes, little is known about how pathways functionally integrate within new hosts. One example of a mobile respiratory metabolism is bacterial chlorate reduction, which is frequently encoded on composite transposons. This implies that the essential components of the metabolism are encoded on these mobile elements. To test this, we heterologously expressed genes for chlorate reduction from *Shewanella algae* ACDC in the non-chlorate-reducing *Shewanella oneidensis* MR-1. The construct that ultimately endowed robust growth on chlorate included *cld*, a cytochrome *c* gene, *clrABDC*, and two genes of unknown function. Although strain MR-1 was unable to grow on chlorate after initial insertion of these genes into the chromosome, 11 derived strains capable of chlorate respiration were obtained through adaptive evolution. Genome resequencing indicated that all of the evolved chlorate-reducing strains replicated a large genomic region containing chlorate reduction genes. Contraction in copy number and loss of the ability to reduce chlorate were also observed, indicating that this phenomenon was extremely dynamic. Although most strains contained more than six copies of the replicated region, a single strain with less duplication also grew rapidly. This strain contained three additional mutations that we hypothesized compensated for the low copy number. We remade the mutations combinatorially in the unevolved strain and determined that a single nucleotide polymorphism (SNP) upstream of *cld* enabled growth on chlorate and was epistatic to a second base pair change in the NarP binding sequence between *narQP* and *nrfA* that enhanced growth.**

IMPORTANCE **The ability of chlorate reduction composite transposons to form functional metabolisms after transfer to a new host is an important part of their propagation. To study this phenomenon, we engineered *Shewanella oneidensis* MR-1 into a chlorate reducer. We defined a set of genes sufficient to endow growth on chlorate from a plasmid, but found that chromosomal insertion of these genes was nonfunctional. Evolution of this inoperative strain into a chlorate reducer showed that tandem duplication was a dominant mechanism of activation. While copy number changes are a relatively rapid way of increasing gene dosage, replicating almost 1 megabase of extra DNA is costly. Mutations that alleviate the need for high copy number are expected to arise and eventually predominate, and we identified a single nucleotide polymorphism (SNP) that relieved the copy number requirement. This study uses both rational and evolutionary approaches to gain insight into the evolution of a fascinating respiratory metabolism.**

Received 18 February 2015 **Accepted** 17 April 2015 **Published** 19 May 2015

Citation Clark IC, Melnyk RA, Youngblut MD, Carlson HK, Iavarone AT, Coates JD. 2015. Synthetic and evolutionary construction of a chlorate-reducing *Shewanella oneidensis* MR-1. mBio 6(3):e00282-15. doi:10.1128/mBio.00282-15.

Editor Stephen J. Giovannoni, Oregon State University

Copyright © 2015 Clark et al. This is an open-access article distributed under the terms of the Creative Commons Attribution-Noncommercial-ShareAlike 3.0 Unported license, which permits unrestricted noncommercial use, distribution, and reproduction in any medium, provided the original author and source are credited.

Address correspondence to John D. Coates, jdcoates@berkeley.edu.

Chlorate (ClO_3^-) is a highly soluble anion hypothesized to form naturally through chlorine photochemistry in the atmosphere (1, 2). Despite having a nonanthropogenic source, environmental contamination is thought to result primarily from the production of bleaching agents and herbicides (3). Chlorate is respired by chlorate-reducing bacteria (CRB) using a series of biochemical steps analogous to those used by perchlorate-reducing bacteria (PRB). The terminal reductase ClrABC first reduces chlorate to chlorite (4), which is converted to chloride and oxygen by chlorite dismutase (Cld) (5).

Numerous CRB and PRB have been isolated, and sequencing efforts have elucidated the genomic architectures of these metabolisms. Comparative analysis has identified shared genetic components and allowed for insight into the evolution of these respiratory pathways (6–8). In contrast to perchlorate reduction genomic islands, chlorate reduction is often encoded on composite transposons (7). The interior of these transposons, which we refer to as the chlorate reduction composite transposon interior (CRI), always contains *clrABDC* and *cld*. In *Shewanella algae* ACDC and *Dechloromarinus chlorophilus* NSS, the CRI also includes a *napC* fragment thought to have been a passenger during the horizontal transfer of a betaproteobacterial *cld* gene (7), as well as a small cytochrome *c* gene, two genes of unknown function, the insertion sequence ISSal*1*, and a gene encoding a methyl-accepting chemotaxis protein (MCP). In two *Pseudomonas* species chlorate reducers, the architecture is very similar, but ISSal*1* and

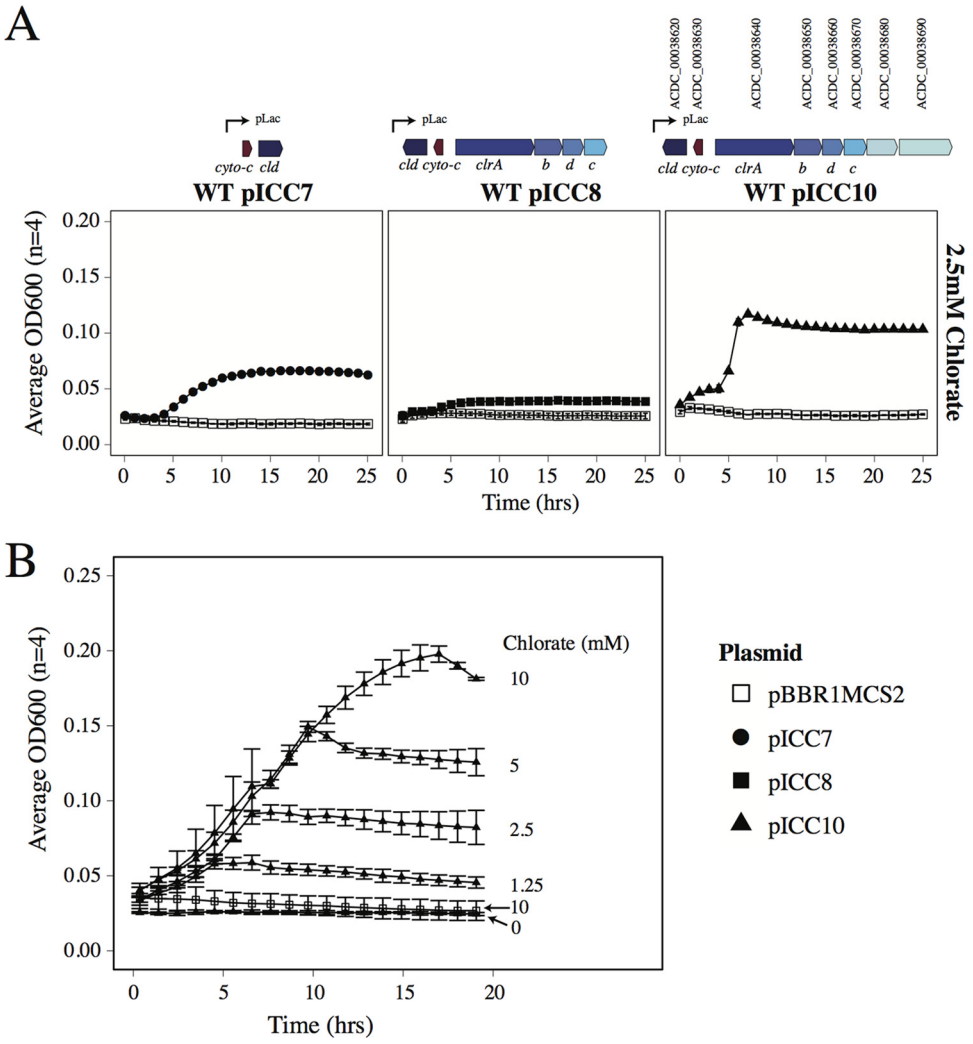

FIG 1 Heterologous expression of genes from the CRI of *Shewanella algae* ACDC in *Shewanella oneidensis* MR-1. (A) Growth of wild-type (WT) *S. oneidensis* MR-1 with plasmids pICC7, pICC8, and pICC10 with empty vector (pBBR1MCS2) controls. (B) Growth of strain MR-1 with pICC10 with increasing concentrations of chlorate demonstrates robust growth.

MCP are absent, while in *Alicycliphilus denitrificans* BC and *Ideonella dechloratans*, genes putatively involved in oxidative stress defense and molybdopterin biosynthesis are also found (6, 7).

The fact that CRIs are encoded on small transposable units suggests that they are often horizontally transferred and that they contain most essential components for chlorate respiration. However, nothing is known about the genetic prerequisites of recipient bacteria, or how the CRI functionally integrates with host systems. An interesting approach to answering these questions is by *de novo* engineering the capacity for chlorate reduction in *Shewanella oneidensis* MR-1. MR-1 reduces numerous electron acceptors using type II dimethyl sulfoxide (DMSO) reductase family enzymes, has the ability to synthesize heme in the presence of oxygen, and contains multiple routes of quinol oxidation, making it an ideal system for such work (9). In this study, we built the capacity for chlorate reduction in strain MR-1, providing insight into mechanisms by which the metabolism functions and evolves after horizontal transfer.

RESULTS AND DISCUSSION

In *trans* expression of the CRI. *Shewanella oneidensis* MR-1 containing a series of plasmids with incrementally larger sections of the CRI from *Shewanella algae* ACDC were tested for growth on chlorate. These plasmids contained (a) *cld* and cytochrome *c* (pICC7: ACDC_00038620-30); (b) *cld*, cytochrome *c*, and *clrABDC* (pICC8: ACDC_00038620-70); or (c) *cld*, cytochrome *c*, *clrABDC*, and two hypothetical genes (pICC10: ACDC_00038620-90). Interestingly, the presence of *cld* and its neighboring cytochrome *c* gene allowed for small but measurable growth (Fig. 1A, leftmost panel), suggesting that an unknown enzyme in the wild-type (WT) strain MR-1 was capable of chlorate turnover and that chlorite detoxification and oxygen production were catalyzed by Cld. No growth was observed on chlorate in an empty vector control. The wide phylogenetic distribution of cytoplasmic Cld-like enzymes, several of which have been functionally characterized (10, 11), suggests that protecting against chlorite is a more general phenomenon than previously thought. Our result implies that inadvertent

chlorate reduction, in the presence of Cld, can actually benefit cells.

Surprisingly, the addition of *clrABDC* to create plasmid pICC8 did not improve growth on chlorate, indicating that *clrABDC* was insufficient. The addition of two conserved genes (ACDC_00038680 and ACDC_00038690), resulting in plasmid pICC10, allowed stronger growth that increased with chlorate concentration (Fig. 1A and B). We conclude that one or both of these genes plays a role during chlorate reduction. ACDC_00038680 is annotated as a MipZ/ParA family protein with an ATPase domain, and ACDC_00038690 is annotated as a glycosyltransferase. These genes are also present downstream of type II DMSO reductases from *Sagittula stellata* E-37 and *Citreicella* sp. strain SE45 in a conserved syntenic arrangement (7).

Evolution of genes sufficient for chlorate reduction into a functional metabolism. With a set of genes sufficient for chlorate reduction defined, we made a single-copy chromosomal insertion of the 11-kb region shown to endow growth on chlorate (ACDC_00038620 to ACDC_00038690) between SO_0910 and SO_0911 in *S. oneidensis* MR-1. This location was selected based on mutant fitness data from Tn-seq experiments, which showed insertions in this region had negligible fitness effects (12). However, the resulting strain (ICC99) could not grow by chlorate reduction. To understand what prevented the metabolism from functioning after chromosomal integration, we provided a strong selective pressure for strain ICC99 to respire chlorate. Cultures were transferred aerobically in the presence of chlorate, and in each transfer, the degree of shaking and headspace volume was reduced. When growth relative to a no-chlorate control was observed, the culture was plated anaerobically with chlorate as the sole electron acceptor, single colonies were selected and placed in anaerobic Hungate tubes, and cultures were transferred until consistent growth on chlorate was established. We resequenced the genomes of 11 strains and searched for single nucleotide polymorphisms (SNPs) and insertions and deletions (indels) (Fig. 2A). Four strains contained mutations in menaquinone biosynthesis: two mutations resulted in a missense mutation in *menA* (Y127N), two caused a *menA* frameshift, and one was a >10-kb deletion that included *menF*. Although menaquinone biosynthesis was disrupted in five strains, there was no correlation between these mutations and growth (Fig. 2B, red). The probability of accumulating three separate types of mutation (frameshift, missense, and deletion) in menaquinone biosynthesis without a selective advantage seemed unlikely, and we postulated that either they provided a fitness benefit during chlorate reduction that was difficult to detect under our experimental conditions, or were somehow advantageous under the microaerophilic conditions used at the start of our evolution experiments. Two strains contained *galU* (SO_1665) mutations, and several other SNPs were identified, but no mutation was shared by all strains, and some strains contained no mutation, suggesting that another mechanism of CRI activation was involved.

We searched for indications of larger structural variation by identifying genomic regions with changes in mapped read coverage and found amplification of 70- to 100-kb regions within all evolved strains (Fig. 2C). Amplification always included *cld* and *clrABDC*, suggesting that it was the target, and that the additional replicated DNA was linked by the amplification mechanism. Growth rate and yield correlated with the fold coverage change, not specific mutations, indicating that this effect was an important part of the ability to reduce chlorate (Fig. 2B). This is consistent with the observation that expression from a multicopy plasmid allowed growth (Fig. 1). Multiple copies of chlorate reduction genes in *Shewanella algae* ACDC were also important for growth on chlorate (13). Except in one case, the amplified region truncated at ISSod*1* insertion sequences, suggesting that unequal recombination at these homologous sequences resulted in tandem duplications (14). Gene amplification as an adaptive process was discovered for the *lac* operon in *Escherichia coli* (14–16), and a system for studying reversion of a Lac$^-$ frameshift during selection on lactose has become a standard tool for interrogating this process. Numerous subsequent examples of tandem duplications occurring during selection for intraintestinal growth (17), carbon source utilization (18), thermal tolerance (19), copper resistance (20), and artificial selectable markers (21) have been demonstrated. From an evolutionary perspective, amplification has several advantages over point mutations: it is orders of magnitude more frequent, is easily reversible, and allows both divergence and maintenance of original function (22).

An SNP upstream of *cld* activates chlorate reduction. Changes in copy number represent a relatively rapid way to tune suboptimal expression, but harboring 600 to 900 kb of extra DNA represents a selective disadvantage. Under aerobic conditions, strains ICC121.1 and ICC121.2 experienced contraction in coverage and lost the ability to grow by chlorate reduction (strains ICC126.1 and ICC126) (Fig. 2). Even under selective conditions, large copy numbers are expected to give way to less frequent point mutations that are free from the cost of excessive DNA replication. One strain (ICC121.10) that contained an average of 2.5-fold chromosomal coverage grew more rapidly than the rate predicted by a regression of growth versus copy number (Fig. 2B, circled strain). This suggested that compensatory mutations allowed more robust growth in the absence of high gene dosage. This strain contained two SNPs and a single base pair insertion that could be responsible for this effect. The SNPs were located between *cld* and cytochrome *c* (SNP1) and between *narQP* (SO_3981 and SO_3982) and *nrfA* (SO_3980) (SNP2), while the indel was found between SO_3718 and SO_3719. To test the importance of the three mutations, we constructed single, double, and triple mutant combinations in the unadapted background (strain ICC99). The mutation upstream of *cld* (SNP1) was sufficient for growth on chlorate, while SNP2 and the indel alone were both insufficient. SNP2 improved growth in an SNP1 background but failed to have an effect in an indel background (Fig. 3A). This indicated that SNP1 was epistatic to SNP2.

SNP1 was upstream of *cld*, and it might change expression of Cld. As such, we compared protein expression of Cld between strains with SNP1 (strains ICC225 and ICC228) and without SNP1 (strain ICC99) using shotgun proteomics (Fig. 3B). Because strain ICC99 did not grow on chlorate, strains were grown on nitrate in order to allow for comparison. Consistent with the role of SNP1 in increasing Cld expression, higher levels of peptides were observed in strains ICC225 and ICC228 than in strain ICC99 (Fig. 3B). SNP1 destabilized a predicted hairpin (23), and it might increase transcriptional read through from the cytochrome *c* gene upstream. However, when the hairpin was deleted in strain ICC99, no growth on chlorate was observed (see Fig. S1 in the supplemental material). This suggests that the mechanism of SNP1 was not related to disruption of a hairpin transcriptional stop.

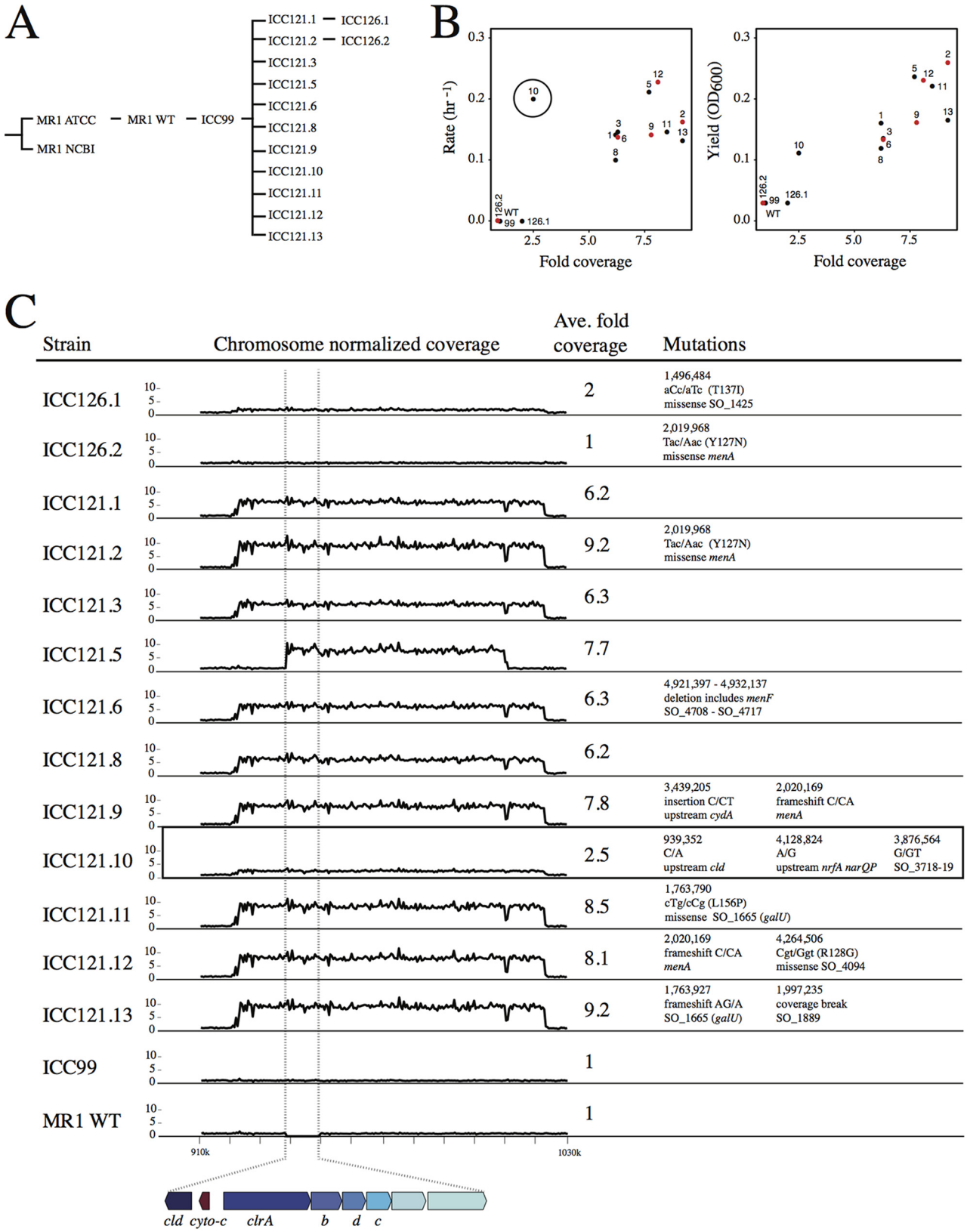

FIG 2 Evolution and resequencing of *Shewanella oneidensis* MR-1. (A) Taxonomic relationship between unevolved and evolved strains used in this study. (B) Correlation between growth and average fold change over chromosomal coverage. Strains with mutations in menaquinone biosynthesis are highlighted in red. The prefix ICC121 has been removed to facilitate data labeling. (C) Plots of reads mapped to a 120-kb region that included *cld* and *clrABDC* and specific SNPs and indels found in each strain.

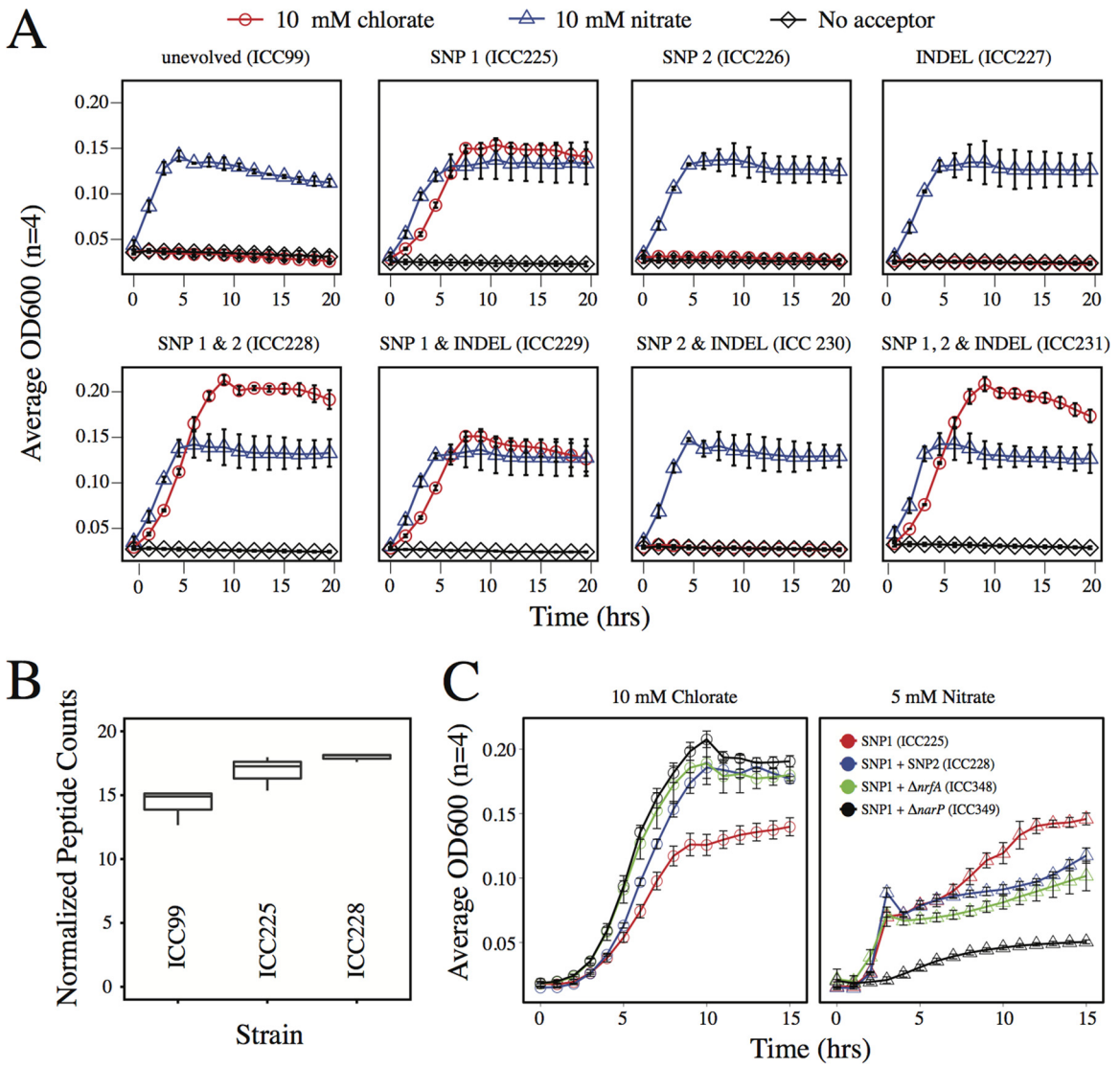

FIG 3 Investigating the roles of specific mutations in activating the chromosomal insertion. (A) Growth of single, double, and triple mutations made in the unevolved strain with 10 mM nitrate as a positive control. (B) Cld protein expression under nitrate-reducing conditions of strains ICC99, ICC225. and ICC228. (C) Investigating the role of SNP2 within the NarP binding sequence between *narQP* and *nrfA*. Growth of strains with mutations SNP1 plus SNP2 (ICC228), SNP1 plus Δ*nrfA* (ICC348), and SNP1 plus Δ*narP* (ICC349) on 10 mM chlorate or 5 mM nitrate.

An SNP between *narQP* and *nrfA* enhances growth on chlorate. SNP2 was upstream of the divergently transcribed two-component system *narQP* and ammonifying nitrite reductase *nrfA* in a highly conserved position at the 3′ end of the predicted NarP binding sequence TACCCCCTAAGAGGT(A>G) (24). NarP is a transcription factor that controls both *nap* and *nrf* operons in *S. oneidensis* MR-1, but it appears to regulate the latter more strongly (25). Given its location within the NarP binding sequence between *narQP* and *nrfA*, SNP2 was likely to influence transcription of one or both of these genes. Indeed, it resulted in decreased growth on 5 mM nitrate, primarily in the second phase of growth that was characteristic of nitrite reduction (Fig. 3C). Deletion of *narP* and *nrfA* in an SNP1 background resulted in increased growth on chlorate (Fig. 3C), almost identically to the effect of SNP2 in that background (strain ICC228). This result hinted at a complex interaction between nitrite and chlorate reduction, which was interesting in light of the fact that *nrfA* was inactivated in *S. algae* ACDC (7).

To understand the role of *nrfA* during chlorate reduction, we tested the ability of the purified enzyme to facilitate chlorate reduction. Using reduced methyl viologen as an electron donor, NrfA was oxidized by 1 mM nitrite, but not chlorate (Fig. 4A). This was not due to inactivation of the enzyme, as nitrite could be subsequently reduced after the addition of chlorate. In addition, chlorate did not inhibit the initial rate of nitrite reduction, even when added at 100 mM concentrations (data not shown). To further confirm this result, we tested the ability of the Δ*nrfA* mutant carrying plasmid pICC7 to grow on chlorate. Deleting *nrfA* did not prevent small amounts of growth on chlorate when *cld* was present (Fig. 5A). We conclude that NrfA does not reduce chlorate. Using NrfA prereduced with methyl viologen and washed to remove the reductant, we monitored the enzyme's UV-visible

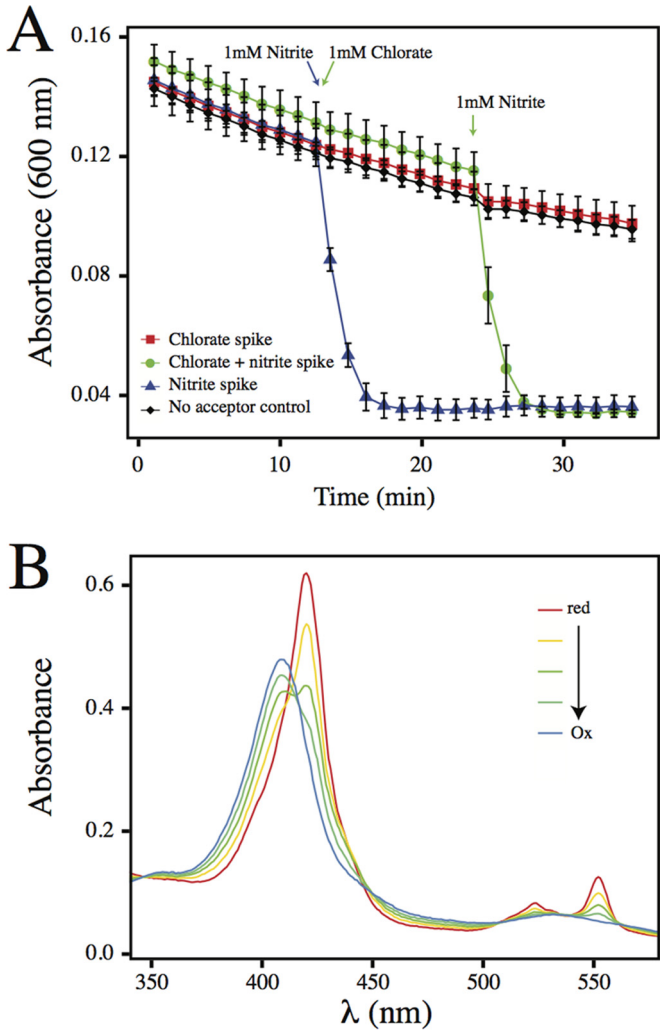

FIG 4 (A) NrfA does not turn over chlorate. Methyl viologen-reduced (MV_{red}) NrfA was spiked first with chlorate, nitrite, or chlorate and then spiked with nitrite or nothing (no-acceptor control). Measurable background MV_{red} oxidation was always observed, but it was not enhanced by the addition of chlorate. (B) Spectroscopy of reduced (red) NrfA demonstrates oxidation (Ox) of the enzyme by chlorite.

(UV-Vis) spectrum after a series of chlorite injections. NrfA was rapidly oxidized by chlorite (Fig. 4B). Reduction of chlorite by NrfA could explain why deletion of this enzyme provided a growth benefit during chlorate reduction: inadvertent reaction with chlorite results in even more toxic chlorine species. However, the exact mechanism of NrfA antagonism as well as the product of oxidation by chlorite remains to be determined.

Interaction of chlorate with the nitrate reduction pathway. As previously described, growth of strain MR-1 on nitrate was characterized by complete reduction of nitrate before the onset of nitrite reduction to ammonium (26). We observed that 10 mM nitrate did not always proceed to nitrite reduction, and 5 mM was used instead. The transition between acceptors was marked by a decrease in growth rate, which allowed the phases to be easily distinguished (Fig. 5B). To further explore the interplay of chlorate and nitrate, we grew wild-type MR-1 in the presence of chlorate. The addition of 2.5 mM chlorate inhibited nitrite reduction and the second phase of growth, introducing *cld* and its neighboring cytochrome *c* gene on a plasmid (pICC7), significantly alleviated the inhibition (Fig. 5B). Ion chromatography confirmed the following. (i) Chlorate inhibited metabolism during the nitrite reduction phase, not the nitrate reduction phase. (ii) pICC7 significantly relieved this inhibition. (iii) A small but measurable turnover of chlorate occurred when pICC7 was introduced (Fig. 5B). This indicated that an enzyme intrinsic to strain MR-1 was capable of reducing chlorate and that Cld was most likely responsible for the resulting chlorite detoxification.

The question remained: what enzyme in wild-type MR-1 was capable of chlorate reduction? To answer this, we used fast protein liquid chromatography to purify chlorate reductase activity from cells grown with nitrate after the transition to ammonification. Fractions with activity were separated by SDS-PAGE, digested in the gel with trypsin, and analyzed by liquid chromatography tandem mass spectrometry. The alpha subunit of the respiratory nitrate reductase NapA (SO_0848) was highly represented in fractions with chlorate reductase activity (see Table S2 in the supplemental material). In contrast to the membrane-bound nitrate reductase (NarGHI) (27–30), the periplasmic nitrate reductase (NapAB) has been reported to not react with chlorate (31–33). To understand whether NapA turnover of chlorate was responsible for the small growth on chlorate observed in the presence of heterologously expressed *cld* (Fig. 1A), we compared the WT strain carrying pICC7 to the Δ*napA* mutant strain carrying pICC7. Deletion of *napA* abolished growth on 2.5 mM chlorate (see Fig. S2 in the supplemental material). These results lead to a model whereby NapA reduces chlorate to chlorite, which subsequently reacts with NrfA. The cycle begins when nitrate is depleted and NapA is free to reduce alternative substrates.

Conclusion. A set of genes sufficient to encode a functional chlorate reduction pathway has been determined via heterologous expression. These genes confer the capacity for chlorate reduction when present at high copy number, either on a plasmid, or when amplified naturally under conditions selecting for growth. This result parallels the copy number requirements observed in *Shewanella algae* ACDC. In the engineered strain MR-1, a single base pair change upstream of the chlorite dismutase alleviated reliance on high copy number and was further enhanced by a second mutation in the NarP binding sequence between *narQP* and *nrfA*. The latter mutation, in conjunction with the observed *nrfA* inactivation in strain ACDC, suggested interplay between ClOx and the nitrate reduction pathway. This was supported by biochemical and genetic evidence for NapA turnover of chlorate and NrfA oxidation by chlorite, raising broader questions about the susceptibility of ammonification to chlorate. This study uses evolution to understand mechanisms by which bacterial chlorate reduction operates after horizontal transfer.

MATERIALS AND METHODS

Media and culture conditions. All experiments were completed in *Shewanella* minimal medium (SMM) at pH 7.2 consisting of, per liter, 1.5 g ammonium chloride, 0.60 g anhydrous sodium phosphate (monobasic), 0.285 g magnesium chloride (anhydrous), 0.10 g potassium chloride, 1.75 g sodium chloride, 7.15 g HEPES, 0.2 g yeast extract, 0.1 g tryptone with vitamins and minerals (34). Growth experiments in which electron acceptors were tracked were completed in anaerobic Hungate tubes with a N_2 headspace at 30°C. Cultures were anaerobically sampled from Hungate tubes, filtered with 0.2-μm syringe filters, and diluted in deionized water. All other growth experiments were completed in flat-bottom 96-well

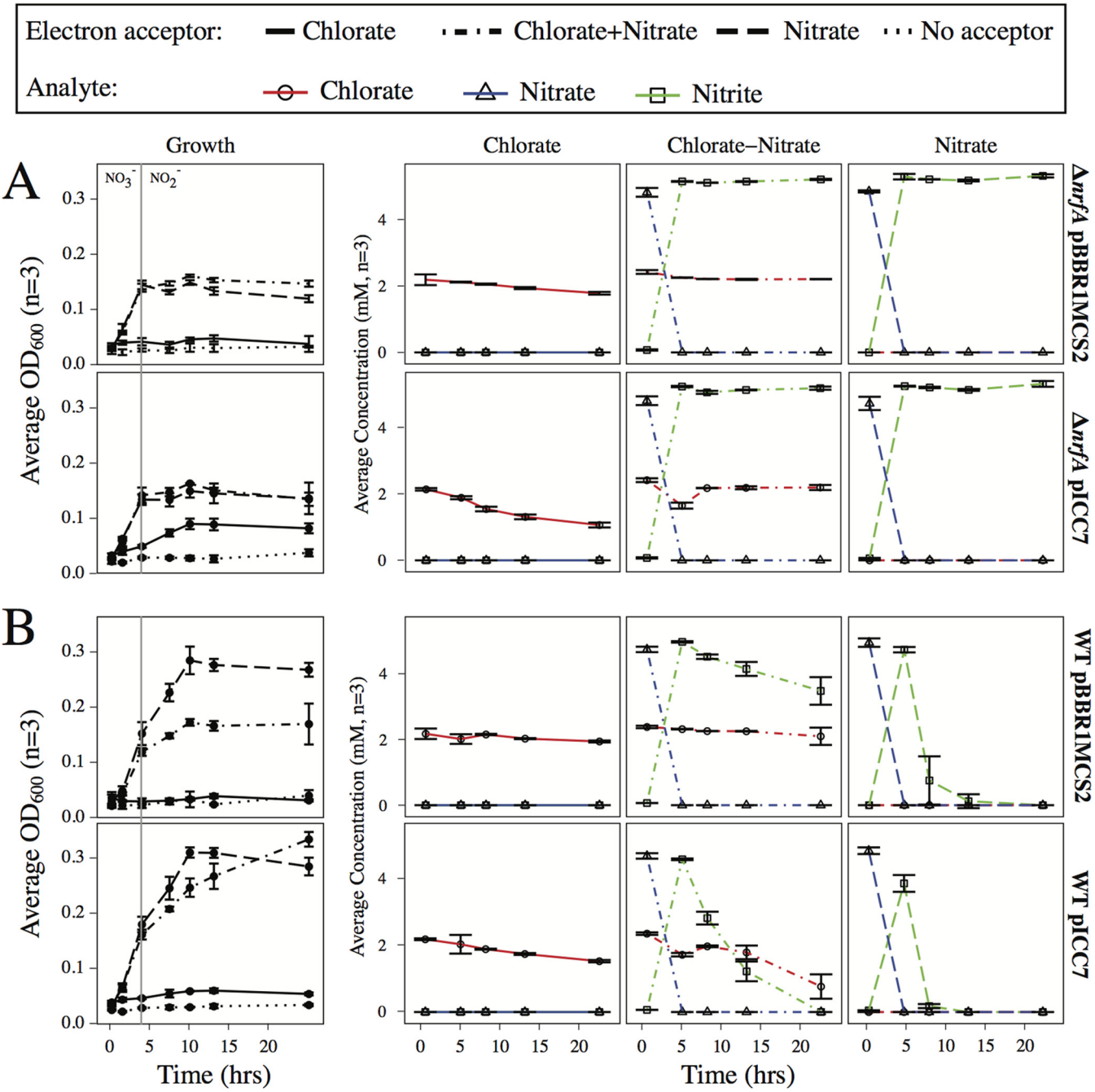

FIG 5 Growth and analyte profiles for cells with different genotypes grown in chlorate alone, chlorate plus nitrate, and nitrate alone demonstrate that (A) *nrfA* is not required for chlorate turnover and that (B) pICC7 rescues chlorate inhibition of nitrite reduction.

plates (Corning Costar, Tewksbury, MA) in an anaerobic chamber (Coy Labs, Grass Lake, MI). The optical density (at 600 nm) was measured with a spectrophotometer (Tecan Sunrise, Männedorf, Switzerland). A total volume of 300 μl was covered with 80 μl of mineral oil and incubated at 30°C without shaking. To test for growth of *Shewanella oneidensis* MR-1 containing various plasmids, cells were pregrown aerobically and inoculated to a starting optical density (600 nm) of 0.03 in anaerobic SMM medium with the appropriate electron acceptor.

Plasmid construction. (i) Expression constructs. PCR with the high-fidelity polymerase Phusion, restriction digestion, and ligation with T4 ligase (NEB) were used to construct three vectors with sequentially larger fractions of the CRI from *Shewanella algae* ACDC in the broad-host-range vector pBBR1MCS2.

(ii) Suicide vector for chromosomal insertion. Approximately 700 bp flanking the insertion site between SO_0910 and SO_0911 were amplified and ligated into the suicide vector pAK31. The resulting vector was digested with AvrII and ligated to an AvrII-cut PCR product containing ACDC_00038620 to ACDC_00038690, creating plasmid pICC30.

(iii) Suicide vectors for in-frame deletions. Approximately 700 bp flanking the gene of interest were amplified and fused with assembly PCR using 5′ linkers added to the internal primers. The assembled product was cloned into a Gateway entry vector and transferred into pAK31GW

(Gateway-compatible *sacB* counterselectable suicide vector) using the LR recombination reaction (Life Technologies). The resulting plasmid was used to generate markerless in-frame deletions.

(iv) Suicide vectors for point mutations and insertions. Amplifying the mutations from the evolved strain ICC121.10 was used to generate suicide vectors with point mutations (SNP1 and SNP2) and a base pair insertion (indel3). The 1-kb products were digested with appropriate restriction enzymes and ligated into pSMV3.

(v) Suicide vectors for the hairpin deletion. PCR with phosphorylated primers was used to generate a deletion of the putative hairpin transcriptional terminator. Primers were phosphorylated with polynucleotide kinase prior to amplification, and the resulting PCR product was self-ligated with T4 ligase (NEB). A list of the primers used and the resulting constructs are found in Table S1 in the supplemental material.

Allelic exchange. Suicide vectors for allelic exchange were transformed into the diaminopimelic acid (DAP) auxotroph *E. coli* WM3064 (W. Metcalf, University of Illinois at Urbana Champaign) and mated with *S. oneidensis* MR-1. Five milliliters of both strains was washed twice in LB, resuspended to an optical density at 600 nm (OD_{600}) of 1, and mixed at a 1:3 (vol/vol) ratio of strain MR-1 to strain WM3064. The mixture was spun (4,000 rpm, 10 min) and spotted on LB supplemented with DAP (300 μg ml^{-1}) (LB-DAP) at 30°C for 8 h. The spot was subsequently suspended in 1 ml LB, diluted 10-fold, and plated on LB with kanamycin (50 μg ml^{-1}). Colonies that appeared within 24 h were patched onto plates containing kanamycin and sucrose (10% [vol/vol]). A single kanamycin-resistant (Km^r) sucrose-sensitive (Suc^s) patch was restreaked and grown overnight in unselective medium, and the resulting outgrowth was plated on sucrose. Colonies that appeared within 24 h were patched onto kanamycin and sucrose, and Km^s Suc^r patches were screened for the desired second crossovers with colony PCR. These patches were streaked, and single colonies were retested by PCR for the appropriate genotype.

Evolution and resequencing. Strain ICC99 was evolved to grow on chlorate by sequentially reducing the oxygen titer with successive transfers in the presence of chlorate. To start, 25 ml of strain ICC99 was shaken at 250 rpm in 50-ml conical tubes with LB and 10 mM chlorate. Each day, 10% of the culture was transferred to a tube containing 5 ml more working volume until, after 5 days, the tube contained 50 ml of liquid. The degree of shaking on an orbital shaker was decreased from 200 rpm to 150, 100, 50, and finally 0 rpm. The unshaken culture was transferred into 50 ml of aerobic LB with 10 mM chlorate until the culture had a higher optical density than the no-chlorate control did. This was plated anaerobically onto SMM with 10 mM acetate and 10 mM chlorate in an anaerobic chamber. Single colonies that appeared within several days were selected, placed in anaerobic SMM medium with 50 mM lactate and 10 mM chlorate, and transferred in Hungate tubes five times to ensure robust growth. Strains that exhibited different growth dynamics were selected for genome resequencing.

Resequencing was performed on a HiSeq2000 sequencing system with 100-bp paired-end reads (QB3 sequencing center, University of California [UC], Berkeley). Adapter contamination was removed using scythe (https://github.com/ucdavis-bioinformatics/scythe), 5′ ends were trimmed by 5 bp with seqtk (https://github.com/lh3/seqtk/), and poor-quality reads were trimmed with sickle (https://github.com/ucdavis-bioinformatics/sickle). Processed reads were mapped to the MR-1 genome sequence (modified to accommodate the CRI insertion) using bwa (35). GATK (36) was used for variant detection as follows: duplicates were marked (MarkDuplicates) and reads were realigned (RealignerTargetCreator and IndelRealigner), before single nucleotide polymorphisms (SNPs) and insertions and deletions (indels) were called with UnifiedGenotyper. SNPs were filtered by quality of depth (QD $<$ 2.0), phred quality (mapping quality score [MQ] $<$ 40), strand bias (Fisher strand filter [FS] $>$ 60), and site consistency (haplotype score $>$ 13). Indels were filtered by quality of depth (QD $<$ 2.0) and strand bias (FS $>$ 120). Genomic coverage was determined after mapping reads using mpileup from SAMtools (37) and plotted over genomic features using custom scripts in R (38).

Analytical techniques. Chlorate, nitrate, and nitrite were measured with an ion chromatograph as previously described (13). NrfA activity assays were performed with methyl viologen (MV) as the electron donor in 50 mM morpholinepropanesulfonic acid (MOPS) buffer (pH 7.2) in an anaerobic chamber (39). Briefly, zinc-reduced MV (75 μM) and 100 pM purified NrfA from *S. oneidensis* MR-1 (a generous gift of the Pacheco lab, University of Wisconsin—Milwaukee) were added to the buffer. The reaction was started upon the addition of substrate (nitrite or chlorate) and reduced MV (MV_{red}) oxidation was monitored by absorbance at 600 nm. Spectroscopy of NrfA was performed after reducing the enzyme with MV, followed by removal of MV_{red} with buffer exchanges in 50 mM MOPS (pH 7.2) (10,000-molecular-weight-cutoff [10K MWCO] protein concentrators; Pierce). One-milliliter cuvettes with reduced protein were spiked with different concentrations (same volume) of degassed chlorite in the anaerobic chamber, mixed in the chamber, sealed in anaerobic cuvettes, and immediately scanned using a spectrophotometer (Cary 50 Bio; Agilent, Santa Clara, CA).

Purification of chlorate reductase activity from nitrate-grown MR-1 strain. Anaerobic purification of chlorate-dependent activity was used to search for the protein involved in chlorate reduction during growth on nitrate. The purification setup consisted of anaerobic buffers within an anaerobic chamber connected to an external fast protein liquid chromatograph (FPLC) (AKTA Explorer; GE Healthcare), which refed to a fraction collector in the anaerobic chamber. Ten liters of wild-type *S. oneidensis* MR-1 grown on 5 mM nitrate was centrifuged (4,000 $\times$ *g*, 15 min), lysed (EmulsiFlex-C3 cell homogenizer; Avestin), ultracentrifuged (150,000 $\times$ *g* for 45 min), and loaded at 3 ml/min onto a 2.5- by 40-cm Q Sepharose FF column (GE Healthcare) preconditioned with anaerobic buffer A (30 mM HEPES, pH 7.5). After the UV-Vis traces on the FPLC detector returned to baseline, proteins were eluted with a linear gradient from 0 to 100% anaerobic buffer B (30 mM HEPES [pH 7.5], 500 mM NaCl) in 300 min. Fractions were tested for chlorate-dependent activity using a phenazine methyl sulfate (PMS)-coupled NAD (NADH) assay as previously described (40). Activity was present between 70 and 80% buffer B. Active fractions were pooled, concentrated in 100-kDa MWCO filters (Amicon) to 500 μl, and loaded at a flow rate of 0.25 ml/min onto a HiPrep Sephacryl S-300 HR size exclusion column (GE Healthcare) equilibrated with anaerobic buffer C (30 mM HEPES [pH 7.5], 150 mM NaCl). Fractions with activity were separated by SDS-PAGE, and bands were cut for proteomics.

Proteomics. (i) Proteomics on whole cells. Strains ICC99, ICC225, and ICC228 were streaked onto LB plates with kanamycin, and single colonies were selected and placed in SMM with kanamycin, 50 mM lactate, and 5 mM nitrate. Cells (50 ml) were harvested in log phase, centrifuged, resuspended, and lysed (550 sonic dismembrator; Fisher Scientific, Waltham, MA) at 4°C. Fifty micrograms of each sample was combined with 0.07% (vol/vol) RapiGest SF surfactant (Waters Corporation, Milford, MA) in 50 mM NH_4HCO_3 at 80°C for 15 min. Samples were incubated with 1 mM dithiothreitol and 1 mM iodoacetamide (Sigma-Aldrich, St. Louis, MO) in two 30-min incubations at room temperature. Samples were proteolyzed overnight with 1:50 trypsin-protein (modified sequencing grade; Promega), incubated at 37°C for 90 min in 0.5% trifluoroacetic acid (TFA) to hydrolyze the RapiGest surfactant, and centrifuged at 14,000 rpm and 6°C for 30 min.

(ii) In-gel digestion and proteomics of SDS-PAGE-separated proteins. Fractions were separated by SDS-PAGE (NuPage 4 to 12% Bis-Tris protein gels [1.5 mm] [10 well]; Novex Life Technologies) with MES buffer (50 mM MES [morpholineethanesulfonic acid], 50 mM Tris base, 0.1% SDS, 1 mM EDTA, pH 7.3) at 200 V for 35 min. Bands of interest were excised and washed for 20 min in 50 mM NH_4HCO_3. Samples were incubated with 1 mM dithiothreitol in 150 μl of 50 mM NH_4HCO_3 for 30 min at 50°C, cooled to room temperature, and incubated with 1 mM iodoacetamide in the dark for 30 min. Gel slices were washed with 500 μl of a 50:50 solution of acetonitrile and 50 mM NH_4HCO_3 for 20 min with shaking. The solvent was discarded, and 50 μl acetonitrile was used to

shrink the fragments, which were dried in a SpeedVac concentrator. Gel pieces were reswelled with 10 μl of 50 mM NH_4HCO_3 containing 0.1 μg trypsin and allowed to digest overnight at 37°C. Supernatant was saved and combined with remaining peptides extracted using 50 μl of 60% acetonitrile with 0.1% formic acid, and a SpeedVac concentrator was used to evaporate the acetonitrile. Liquid chromatography coupled to tandem mass spectrometry of trypsin-digested samples was performed as previously described (41), except as follows. Solvent A was 99.9% water−0.1% formic acid, and solvent B was 99.9% acetonitrile−0.1% formic acid (vol/vol). The elution program consisted of isocratic flow at 2% solvent B for 4 min, a linear gradient to 30% solvent B over 38 min, isocratic flow at 95% solvent B for 6 min, and isocratic flow at 2% solvent B for 12 min, at a flow rate of 300 nl min^{-1}. Full-scan mass spectra were acquired over the range m/z = 350 to 1,800. In the data-dependent mode, the eight most intense ions exceeding an intensity threshold of 20,000 counts were selected from each full-scan mass spectrum for tandem mass spectrometry (MS/MS). Raw data were searched against the *Shewanella oneidensis* MR-1 protein database using Proteome Discoverer software (version 1.3, SEQUEST algorithm; Thermo) for tryptic peptides (i.e., peptides resulting from cleavage at the C-terminal end of lysine and arginine residues) with up to three missed cleavages and carbamidomethylcysteine and methionine sulfoxide as variable posttranslational modifications. A decoy database was used to characterize the false discovery rate, and the target false discovery rate was 0.01 (i.e., 1%).

SUPPLEMENTAL MATERIAL

Supplemental material for this article may be found at http://mbio.asm.org/lookup/suppl/doi:10.1128/mBio.00282-15/-/DCSupplemental.

Figure S1, TIF file, 2.7 MB.
Figure S2, TIF file, 2.7 MB.
Table S1, XLS file, 0.05 MB.
Table S2, XLSX file, 2.1 MB.

ACKNOWLEDGMENTS

Funding for research on perchlorate and chlorate reduction in the laboratory of J.D.C. has been provided through the Energy Biosciences Institute, University of California, Berkeley. The Vincent J. Coates Genomics Sequencing Laboratory at UC Berkeley, supported by NIH S10 instrumentation grants S10RR029668 and S10RR027303.418, was used in this study. The Computational Genomics Resource Laboratory, which is part of the California Institute for Quantitative Biosciences, was used for computational analysis.

The funders had no role in study design, data collection and analysis, decision to publish, or preparation of the manuscript.

REFERENCES

1. **Rao B, Hatzinger PB, Böhlke JK, Sturchio NC, Andraski BJ, Eckardt FD, Jackson WA**. 2010. Natural chlorate in the environment: application of a new IC-ESI/MS/MS method with a $Cl^{18}O_3^-$ internal standard. Environ Sci Technol **44:**8429–8434. http://dx.doi.org/10.1021/es1024228.
2. **Kang N, Anderson TA, Jackson WA**. 2006. Photochemical formation of perchlorate from aqueous oxychlorine anions. Anal Chim Acta **567:**48–56. http://dx.doi.org/10.1016/j.aca.2006.01.085.
3. **Gordon G, Tachiyashiki S**. 1991. Kinetics and mechanism of formation of chlorate ion from the hypochlorous acid/chlorite ion reaction at pH 6-10. Environ Sci Technol **25:**468–474. http://dx.doi.org/10.1021/es00015a014.
4. **Wolterink AF, Schiltz E, Hagedoorn PL, Hagen WR, Kengen SW, Stams AJ**. 2003. Characterization of the chlorate reductase from *Pseudomonas chloritidismutans*. J Bacteriol **185:**3210–3213. http://dx.doi.org/10.1128/JB.185.10.3210-3213.2003.
5. **van Ginkel CG, Rikken GB, Kroon AG, Kengen SW**. 1996. Purification and characterization of chlorite dismutase: a novel oxygen-generating enzyme. Arch Microbiol **166:**321–326. http://dx.doi.org/10.1007/s002030050390.
6. **Thorell HD, Stenklo K, Karlsson J, Nilsson T**. 2003. A gene cluster for chlorate metabolism in *Ideonella dechloratans*. Appl Environ Microbiol **69:**5585–5592. http://dx.doi.org/10.1128/AEM.69.9.5585-5592.2003.
7. **Clark IC, Melnyk RA, Engelbrektson A, Coates JD**. 2013. Structure and evolution of chlorate reduction composite transposons. mBio **4**(4):e00379-13. http://dx.doi.org/10.1128/mBio.00379-13.
8. **Melnyk RA, Engelbrektson A, Clark IC, Carlson HK, Byrne-Bailey K, Coates JD**. 2011. Identification of a perchlorate reduction genomic island with novel regulatory and metabolic genes. Appl Environ Microbiol **77:**7401–7404. http://dx.doi.org/10.1128/AEM.05758-11.
9. **Hau HH, Gralnick JA**. 2007. Ecology and biotechnology of the genus *Shewanella*. Annu Rev Microbiol **61:**237–258. http://dx.doi.org/10.1146/annurev.micro.61.080706.093257.
10. **Kostan J, Sjöblom B, Maixner F, Mlynek G, Furtmüller PG, Obinger C, Wagner M, Daims H, Djinović-Carugo K**. 2010. Structural and functional characterisation of the chlorite dismutase from the nitrite-oxidizing bacterium "*Candidatus Nitrospira defluvii*": identification of a catalytically important amino acid residue. J Struct Biol **172:**331–342. http://dx.doi.org/10.1016/j.jsb.2010.06.014.
11. **Mlynek G, Sjöblom B, Kostan J, Füreder S, Maixner F, Gysel K, Furtmüller PG, Obinger C, Wagner M, Daims H, Djinović-Carugo K**. 2011. Unexpected diversity of chlorite dismutases: a catalytically efficient dimeric enzyme from *Nitrobacter winogradskyi*. J Bacteriol **193:**2408–2417. http://dx.doi.org/10.1128/JB.01262-10.
12. **Deutschbauer A, Price MN, Wetmore KM, Shao W, Baumohl JK, Xu Z, Nguyen M, Tamse R, Davis RW, Arkin AP**. 2011. Evidence-based annotation of gene function in *Shewanella oneidensis* MR-1 using genome-wide fitness profiling across 121 conditions. PLoS Genet **7:**e1002385. http://dx.doi.org/10.1371/journal.pgen.1002385.
13. **Clark IC, Melnyk RA, Iavarone AT, Novichkov PS, Coates JD**. 2014. Chlorate reduction in Shewanella algae ACDC is a recently acquired metabolism characterized by gene loss, suboptimal regulation and oxidative stress. Mol Microbiol **94:**107–125. http://dx.doi.org/10.1111/mmi.12746.
14. **Anderson RP, Roth JR**. 1977. Tandem genetic duplications in phage and bacteria. Annu Rev Microbiol **31:**473–505. http://dx.doi.org/10.1146/annurev.mi.31.100177.002353.
15. **Horiuchi T, Horiuchi S, Novick A**. 1963. The genetic basis of hypersynthesis of beta-galactosidase. Genetics **48:**157–169.
16. **Tlsty TD, Albertini AM, Miller JH**. 1984. Gene amplification in the *lac* region of *E. coli*. Cell **37:**217–224. http://dx.doi.org/10.1016/0092-8674(84)90317-9.
17. **Mekalanos JJ**. 1983. Duplication and amplification of toxin genes in *Vibrio cholerae*. Cell **35:**253–263. http://dx.doi.org/10.1016/0092-8674(83)90228-3.
18. **Zhong S, Khodursky A, Dykhuizen DE, Dean AM**. 2004. Evolutionary genomics of ecological specialization. Proc Natl Acad Sci U S A **101:**11719–11724. http://dx.doi.org/10.1073/pnas.0404397101.
19. **Riehle MM, Bennett AF, Long AD**. 2001. Genetic architecture of thermal adaptation in *Escherichia coli*. Proc Natl Acad Sci U S A **98:**525–530. http://dx.doi.org/10.1073/pnas.021448998.
20. **Fogel S, Welch JW**. 1982. Tandem gene amplification mediates copper resistance in yeast. Proc Natl Acad Sci U S A **79:**5342–5346. http://dx.doi.org/10.1073/pnas.79.17.5342.
21. **Jannière L, Niaudet B, Pierre E, Ehrlich SD**. 1985. Stable gene amplification in the chromosome of *Bacillus subtilis*. Gene **40:**47–55. http://dx.doi.org/10.1016/0378-1119(85)90023-X.
22. **Hastings PJ, Bull HJ, Klump JR, Rosenberg SM**. 2000. Adaptive amplification: an inducible chromosomal instability mechanism. Cell **103:**723–731. http://dx.doi.org/10.1016/S0092-8674(00)00176-8.
23. **Zuker M**. 2003. mfold web server for nucleic acid folding and hybridization prediction. Nucleic Acids Res **31:**3406–3415. http://dx.doi.org/10.1093/nar/gkg595.
24. **Novichkov PS, Kazakov AE, Ravcheev DA, Leyn SA, Kovaleva GY, Sutormin RA, Kazanov MD, Riehl W, Arkin AP, Dubchak I, Rodionov DA**. 2013. RegPrecise 3.0 − a resource for genome-scale exploration of transcriptional regulation in bacteria. BMC Genomics **14:**745. http://dx.doi.org/10.1186/1471-2164-14-745.
25. **Dong Y, Wang J, Fu H, Zhou G, Shi M, Gao H**. 2012. A Crp-dependent two-component system regulates nitrate and nitrite respiration in *Shewanella oneidensis*. PLoS One **7:**e51643. http://dx.doi.org/10.1371/journal.pone.0051643.
26. **Cruz-García C, Murray AE, Klappenbach JA, Stewart V, Tiedje JM**. 2007. Respiratory nitrate ammonification by *Shewanella oneidensis* MR-1. J Bacteriol **189:**656–662. http://dx.doi.org/10.1128/JB.01194-06.
27. **Marangon J, Paes de Sousa PM, Moura I, Brondino CD, Moura JJG, González PJ**. 2012. Substrate-dependent modulation of the enzymatic

catalytic activity: reduction of nitrate, chlorate and perchlorate by respiratory nitrate reductase from *Marinobacter hydrocarbonoclasticus* 617. Biochim Biophys Acta **1817:**1072–1082. http://dx.doi.org/10.1016/j.bbabio.2012.04.011.

28. **Stewart V**. 1988. Nitrate respiration in relation to facultative metabolism in enterobacteria. Microbiol Rev **52:**190–232.
29. **Ridley H, Watts CA, Richardson DJ, Butler CS**. 2006. Resolution of distinct membrane-bound enzymes from *Enterobacter cloacae* SLD1a-1 that are responsible for selective reduction of nitrate and selenate oxyanions. Appl Environ Microbiol **72:**5173–5180. http://dx.doi.org/10.1128/AEM.00568-06.
30. **Afshar S, Johnson E, de Vries S, Schröder I**. 2001. Properties of a thermostable nitrate reductase from the hyperthermophilic archaeon *Pyrobaculum aerophilum*. J Bacteriol **183:**5491–5495. http://dx.doi.org/10.1128/JB.183.19.5491-5495.2001.
31. **Butler CS, Charnock JM, Bennett B, Sears HJ, Reilly AJ, Ferguson SJ, Garner CD, Lowe DJ, Thomson AJ, Berks BC, Richardson DJ**. 1999. Models for molybdenum coordination during the catalytic cycle of periplasmic nitrate reductase from *Paracoccus denitrificans* derived from EPR and EXAFS spectroscopy. Biochemistry **38:**9000–9012. http://dx.doi.org/10.1021/bi990402n.
32. **Bell LC, Richardson DJ, Ferguson SJ**. 1990. Periplasmic and membrane-bound respiratory nitrate reductases in *Thiosphaera pantotropha*. The periplasmic enzyme catalyzes the first step in aerobic denitrification. FEBS Lett **265:**85–87. http://dx.doi.org/10.1016/0014-5793(90)80889-Q.
33. **Sears HJ, Ferguson SJ, Richardson DJ, Spiro S**. 1993. The identification of a periplasmic nitrate reductase in *Paracoccus denitrificans*. FEMS Microbiol Lett **113:**107–111. http://dx.doi.org/10.1111/j.1574-6968.1993.tb06496.x.
34. **Bruce RA, Achenbach LA, Coates JD**. 1999. Reduction of (per)chlorate by a novel organism isolated from paper mill waste. Environ Microbiol **1:**319–329. http://dx.doi.org/10.1046/j.1462-2920.1999.00042.x.
35. **Li H, Durbin R**. 2009. Fast and accurate short read alignment with Burrows-Wheeler transform. Bioinformatics **25:**1754–1760. http://dx.doi.org/10.1093/bioinformatics/btp324.
36. **DePristo MA, Banks E, Poplin R, Garimella KV, Maguire JR, Hartl C, Philippakis AA, del Angel G, Rivas MA, Hanna M, McKenna A, Fennell TJ, Kernytsky AM, Sivachenko AY, Cibulskis K, Gabriel SB, Altshuler D, Daly MJ**. 2011. A framework for variation discovery and genotyping using next-generation DNA sequencing data. Nat Genet **43:**491–498. http://dx.doi.org/10.1038/ng.806.
37. **Li H, Handsaker B, Wysoker A, Fennell T, Ruan J, Homer N, Marth G, Abecasis G, Durbin R, 1000 Genome Project Data Processing Subgroup**. 2009. The Sequence Alignment/Map format and SAMtools. Bioinformatics **25:**2078–2079. http://dx.doi.org/10.1093/bioinformatics/btp352.
38. **R Core Team**. 2013. R: a language and environment for statistical computing, 3rd ed. R Foundation for Statistical Computing, Vienna, Austria.
39. **Youngblut M, Judd ET, Srajer V, Sayyed B, Goelzer T, Elliott SJ, Schmidt M, Pacheco AA**. 2012. Laue crystal structure of *Shewanella oneidensis* cytochrome *c* nitrite reductase from a high-yield expression system. J Biol Inorg Chem **17:**647–662. http://dx.doi.org/10.1007/s00775-012-0885-0.
40. **Heinnickel M, Smith SC, Koo J, O'Connor SM, Coates JD**. 2011. A bioassay for the detection of perchlorate in the ppb range. Environ Sci Technol **45:**2958–2964. http://dx.doi.org/10.1021/es103715f.
41. **Jinek M, Jiang F, Taylor DW, Sternberg SH, Kaya E, Ma E, Anders C, Hauer M, Zhou K, Lin S, Kaplan M, Iavarone AT, Charpentier E, Nogales E, Doudna JA**. 2014. Structures of Cas9 endonucleases reveal RNA-mediated conformational activation. Science **343:**1247997. http://dx.doi.org/10.1126/science.1247997.